Heliyon 7 (2021) e08024

Contents lists available at ScienceDirect

Heliyon

journal homepage: www.cell.com/heliyon

Research article

Trend and change-point detection analyses of rainfall and temperature over the Awash River basin of Ethiopia

Yitea Seneshaw Getahun [a,b,c,*], Ming-Hsu Li [b], Iam-Fei Pun [b]

[a] Taiwan International Graduate Program (TIGP), Earth System Science Program, Academia Sinica, Taipei, 115, Taiwan
[b] Graduate Institute of Hydrological and Oceanic Sciences, National Central University, Taoyuan, 320, Taiwan
[c] College of Agriculture and Natural Resource Sciences, Debre Berhan University, Debre Berhan, 445, Ethiopia

ARTICLE INFO

Keywords:
Sea surface temperature anomalies
Rainfall variability
Change-point detection
Trend analysis

ABSTRACT

Awash River basin (ARB) as a system is in a state of continuous change that requires successive studies to discern the changes or trends of climatic elements through time due to climate change/variability, and other socio-economical developmental activities in the basin. The livelihood of communities in the ARB is primarily based on rainfall-dependent agriculture. Effects of rainfall anomalies such as reduction of agricultural productivity, water scarcity, and food insecurity are becoming more prevalent in this area. In recent years, ARB has been experiencing more frequent rainfall anomalies that change-point detection test and trend analyses of basin rainfall associated with sea surface temperature is crucial in providing guidance to improve agricultural productivity in ARB. Change-point detection tests such as Pettit's, the von Neumann ratio (VNR), Buishand's range (BR) and standard normal homogeneity (SNH) plus trend analysis Mann-Kendall (MK) test of rainfall and temperature data from 29 meteorological stations in the ARB were carried out from 1986 to 2016. A significant increasing trend of annual and seasonal temperature was found. The temperature change-points for the annual and major rainy season (MRS) were detected in 2001, while for the minor rainy season (mRS) in 1997. A significant decreasing trend, shift, and high variability of rainfall were detected in the downstream part of the ARB. The BR and SNH results showed that the mRS rainfall change-point was in 1998, with a subsequent mean annual decrease of 52.5 mm. The increase (decrease) of rainfall in the annual and MRS was attributable to La Niña (El Niño) events. The significant decreasing trend and change-point of rainfall in the mRS was attributable to the steady warming of the Indian and Atlantic Oceans, local warming, and La Niña events. With this knowledge of the current trends and change-point for rainfall and temperature in the ARB, it is therefore essential that appropriate integrated water management and water-harvesting technologies are established, especially in the downstream areas. Moreover, early detection of El Niño episodes would provide invaluable warning of impending rainfall anomalies in the ARB and would enable better preparations to mitigate its negative effects.

1. Introduction

In recent decades, several studies have reported the effects of climate change/variability as manifested by the increasing rainfall anomalies and temperature (Ramli et al., 2019; Asfaw et al., 2018; Alemayehu and Bewket, 2017). The rising global temperature attributed to the greenhouse gases emission is unequivocal that in turn affects the rainfall anomalies (IPCC, 2014). Rainfall amount is expected to decrease while its anomaly is likely to increase in the Sub-Saharan Africa (IPCC, 2014). Current studies of climate change/variability have been mostly focusing on basin scale that provides more detail information for a better management and planning of local resources (Ramli et al., 2019; Elsanabary and Gan, 2015).

The economy of Awash River Basin (ARB) in Ethiopia is highly reliant on rain-fed agriculture that is vastly sensitive to changes and variability of climate (Borgomeo et al., 2018). Rainfall anomalies tend to lower the agricultural productivity, livestock production, food security, and water availability of ARB (Tilahun et al., 2011). Thus, the expanding agricultural sector in the ARB is particularly vulnerable to rainfall anomalies and a decrease in the rainfall scenario can lead to a 5% decline in the basin's gross domestic product (GDP), with agricultural GDP possibly decreasing by as much as 10% (Borgomeo et al., 2018). In the future, climate variability is likely to worsen the water scarcity in the Sub-Saharan Africa

* Corresponding author.
E-mail address: yiseneshaw@g.ncu.edu.tw (Y.S. Getahun).

https://doi.org/10.1016/j.heliyon.2021.e08024
Received 26 July 2021; Received in revised form 27 August 2021; Accepted 15 September 2021

(IPCC, 2014). The effects of climate variability in the ARB is likely to be widespread due to ARB's high population, and is the most utilized river basin in Ethiopia that contributes greatly to the development of the national economy (Hailu et al., 2017; Bekele et al., 2017). Water scarcity has increased due to rapid population growth, urbanization, and climate variability that induces unreliable rainfall, which further results in recurring droughts (Hailu et al., 2017; Adeba et al., 2015). The water deficit has been severe in recent years, and it has affected development activities as well as the livelihoods of communities within the basin. Therefore, investigation of long-term trends and variation of rainfall and temperature in the ARB is of vital importance for managing of water resources and predicting weather-related disasters.

Furthermore, the predictive accuracy of climate, weather, and hydrological studies is depends on the quality of historical climate datasets (Javari, 2016; Ros et al., 2015). Pitifully, a number of non-climatic factors such as war, meteorological station relocation, failure of meteorological instruments, mishandling of data and abrupt environmental changes can affect the quality of historical climate data, leading to unrealistic trends, shifts, or jumps in the data record that can introduce errors into further analyses (Ros et al., 2015). Hence, understanding factors that affect the quality of historical climate data is vital for performing accurate climate change and variability studies. Change-point detection and trend analysis of rainfall and temperature is vital for the successive better studies of climate change/variability (Bisai et al., 2014; Jain et al., 2013).

Change-point detection of climate data have been performed using Buishand's range (BR), standard normal homogeneity (SNH), Pettit's and the von Neumann ratio (VNR) tests besides to the trend analysis based on Mann-Kendall (MK) test (Suhaila and Yusop, 2018; Onyutha, 2016; Javari, 2016; Jaiswal et al., 2015; Zarenistanak et al., 2014; Croitoru et al., 2012). The Manna Kendall Trend test of rainfall and temperature has been conducted in different part of Ethiopia (Demissie and Sime, 2021; Wedajo et al., 2019; Samy et al., 2019; Elzeiny et al., 2019; Asfaw et al., 2018; Alemayehu and Bewket, 2017; Hayelom et al., 2017; Tamiru et al., 2015; Mengistu et al., 2014) and Awash river basin (Shawul and Chakma, 2020; Mulugeta et al., 2019; Gedefaw et al., 2018; Bekele et al., 2017). These above several recent studies in Ethiopia showed a significantly increasing trend in temperature and an inconsistent trend in rainfall. The above studies in ARB applied MK test for rainfall, and streamflow analyses but not for temperature, excluding Gedefaw et al. (2018) that used stations in the upper part of ARB, which were not adequate and representative of the entire ARB. Location information of all the stations in Gedefaw et al. (2018) were wrongly displayed and even with the correct location some of the station are quite far from ARB. Additionally, most of the previous studies were carried out in the upper part of the ARB, although the spatiotemporal distribution of rainfall and temperature over the basin is extremely uneven. In other words, the downstream part of ARB has not been well investigated. Furthermore, none of the previous studies has performed change-point detection tests. This means that there still exists lack of proper understanding of past temperature and rainfall in the ARB for different time series. Thus, a comprehensive study that incorporates large-scale climate indexes (Sea Surface Temperature Anomalies) such as El Niño–Southern Oscillation (ENSO), the Dipole Moment of Indian Ocean (DMI), the Atlantic Multi-decadal Oscillation (AMO), and the North Atlantic Tropical Index (NTA) is crucial in order to have a better picture on variation trends of temperature and rainfall in the ARB.

It has been shown that the rainfall in the major rainy season (MRS) in Ethiopia (June–September) declines during an El Niño event and increases during a La Niña event (Le et al., 2020; Degefu et al., 2017; Gleixner et al., 2016; Onyutha et al., 2016; Fekadu, 2015; Elsanabary and Gan, 2015; Zaroug et al., 2014; Berhane et al., 2014; Abtew et al., 2009). Moreover, the correlation strength of large-scale climate indexes with rainfall varies from season to season and region to region, and their complexity is not well understood. Thus, basin scale studies will enhance the predictability of seasonal rainfall. Assessments of large-scale climate indexes relating to rainfall pattern have been performed across the Ethiopia, but to date there has been no specific study on the ARB.

The main objective of this study was to examine trends and perform change-point detection tests on rainfall and temperature data of ARB. The change-point detection tests were carried out using Pettit's, VNR, BR, and SNH tests, while a MK trend test was used for trend analysis.

The influence of elevation and large-scale climate indexes on the rainfall of the ARB were also examined, with the climate indexes used being ENSO, DMI, AMO, and NTA.

An attempt was made in this paper to deliver a comprehensive interpretation of trends and shifts in seasonal and annual mean rainfall in the ARB in relation to local and global climatic drivers. It was concluded that mRS rainfall has shifted and shows a significantly decreasing trend, particularly in the downstream area of the basin. It is therefore crucial that to improve water-resource management strategies and identify better adaptation options for the expanding agricultural activities in the ARB.

2. Study area description and data

2.1. Study area description

Awash River has a length of 1,200 km, and it has a drainage area of 116,374 km^2. The elevation of ARB varies from 215 m to 4185 m (Figure 1). The Awash River originates from the central uplands, which lie west of capital city (Addis Ababa) at an elevation of 3,000 m, and terminates in Lake Abbe at an elevation of 215 m, near the border with Djibouti (Dost et al., 2013). Approximately 18 million people and 6 million livestock are estimated to dwell within the ARB (Hailu et al., 2017; Dost et al., 2013), making it the most heavily exploited river basin in Ethiopia due to the existence of major industries, larger cities, and higher populations in the ARB than in other regions of the country (Adeba et al., 2015). The total mean yearly volume of surface water available in ARB is estimated to be 4.64 billion m^3 (Adeba et al., 2015).

The climate of ARB ranges from humid subtropical in the upstream as well as southern and northwestern peripheries of the basin to an arid climate over the eastern lowlands of the basin (Murendo et al., 2010). The mean annual temperature varies from 10 °C in the upstream as well as southern and northwestern peripheries of the basin to 30.5 °C in the eastern lowlands of the basin (Adeba et al., 2015). Based on data from 1986-2016, the mean annual rainfall varies from 900-1300 mm in the upstream and northwestern peripheries of the basin to 192–500 mm in the eastern lowlands of the basin (Figure 2). In general, there are three seasons in Ethiopia/ARB: (1) the major rainy season (MRS), locally called “Kiremt” during June, July, August, and September (JJAS), (2) the minor rainy season (mRS), locally called “Belg” during February, March, April and May (FMAM) and (3) the dry season, also known as “Bega” during October, November, December and January (ONDJ) (Degefu et al., 2017; Fekadu, 2015). The high rainfall areas either for MRS or mRS are associated with elevation.

2.2. Datasets

The observed monthly temperature and rainfall datasets from 1986-2016 for 31 years were obtained from 29 meteorological stations of the National Meteorological Agency (NMA), Ethiopia (Figure 2). Pre-processed and quality checked monthly temperature and rainfall data were collected from NMA. Meteorological stations with the longest recorded data, communal period of record data with other stations and better quality of data were chosen for analyses. The sea surface temperature anomalies (SSTAs), namely the AMO (50°-60°N, 10–50°W), the NTA (5.5°-23.5°N, 15°- 57.5°W), and Niño 3.4 (170°- 120°W, 5°N-5°S) were downloaded from the National Oceanic and Atmospheric Administration (NOAA) website (https://www.esrl.noaa.gov/psd/data/timeseries/AMO/). AMO is characterized in two ways that the first one comprises detrended SSTA averaged over the North Atlantic from 0°-70°N, to

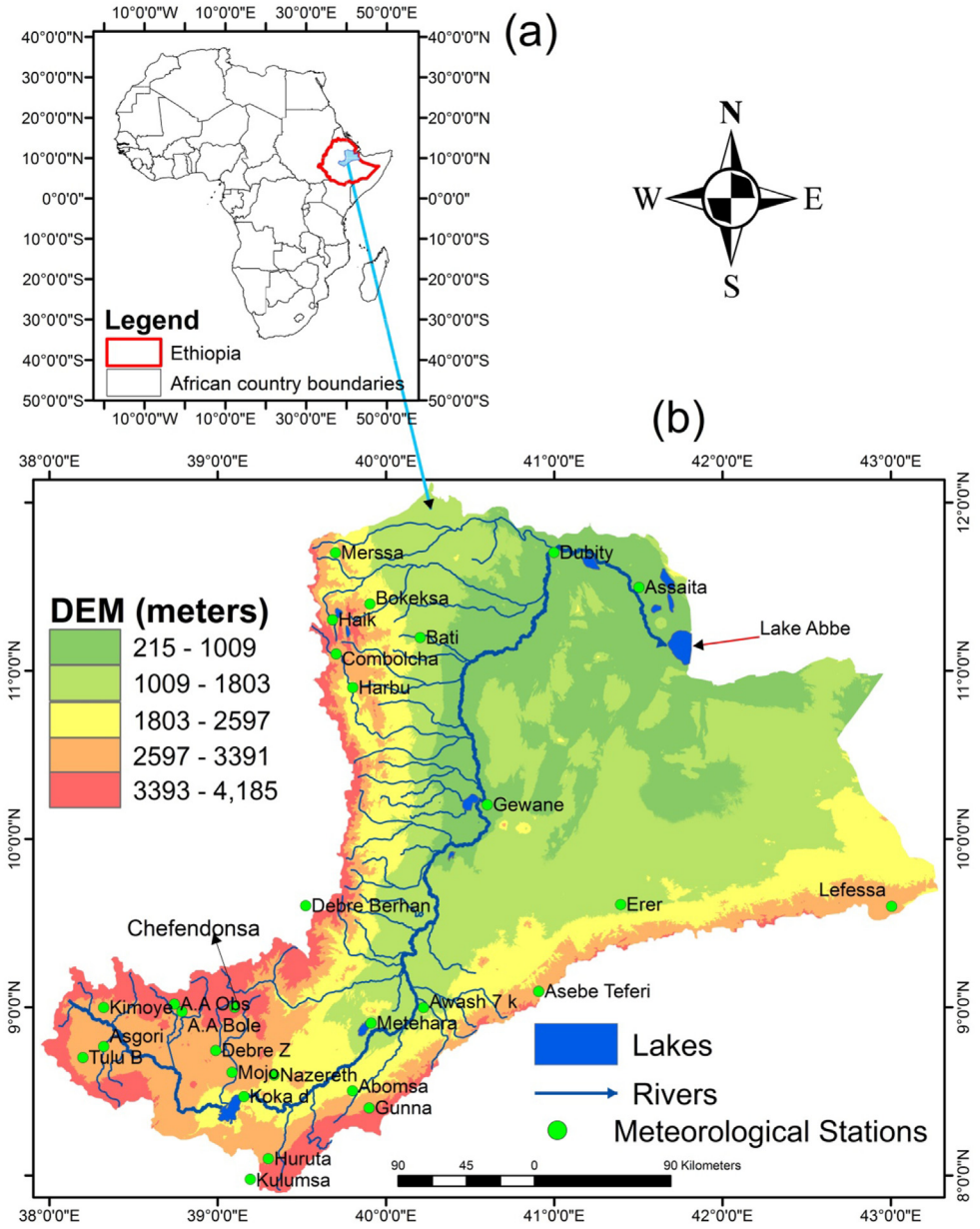

Figure 1. Map of the study area: a) Africa, Ethiopia (Awash river basin), b) meteorological stations used for this study, DEM, Lakes and major rivers of ARB.

remove global warming signals and obtain a pure oscillatory signal of the Atlantic sea surface temperature (SST). The second comprises the North Atlantic SST data with the global mean SST data subtracted to remove global effect signals (Park and Li., 2018; Marullo et al., 2011; Trenberth and Shea, 2006). In this study, the first ways were used to remove the global warming signal from other SSTA series (Hong et al., 2008). The DMI is the difference in SSTAs between the eastern (90°–110ºE, 10ºS to 0ºN) and western (50°–70ºE and 10°S to 10°N) tropical Indian Ocean, which was obtained from the Japan Agency for Marine Earth Science and Technology (http://www.jamstec.go.jp/frsgc/research/d1/iod/e/iod/dipole_mode_index.html).

3. Methodology

3.1. Average rainfall and temperature for the entire basin

The entire basin average areal rainfall and temperature were calculated using Thiessen polygon method via ArcGIS. The Thiessen polygon approach gives weight to station data in proportion to the space between the stations. To determine the mean rainfall or temperature, the rainfall or temperature amount of each station (X_i) is multiplied by the area of its polygon (A_s) and the sum of the products is divided by the total area (A). The areal rainfall and temperature were computed from the monthly point measurement of rainfall or temperature within and around Awash River basin by Thiessen polygon method.

$$P_{avg} = \frac{1}{A}\sum_{i=1}^{n}(A_s * y_i) \quad (1)$$

where, P_{avg}: Areal average rainfall (mm/month), Y_i: rainfall measured at sub-region (mm/month), A_s: Area of sub-region (km^2), and A: total area of sub regions (km^2).

3.2. Coefficients of variation (CV) for rainfall

The measure of how much the rainfall amount deviated from the mean is coefficient of variation. The CV was calculated as

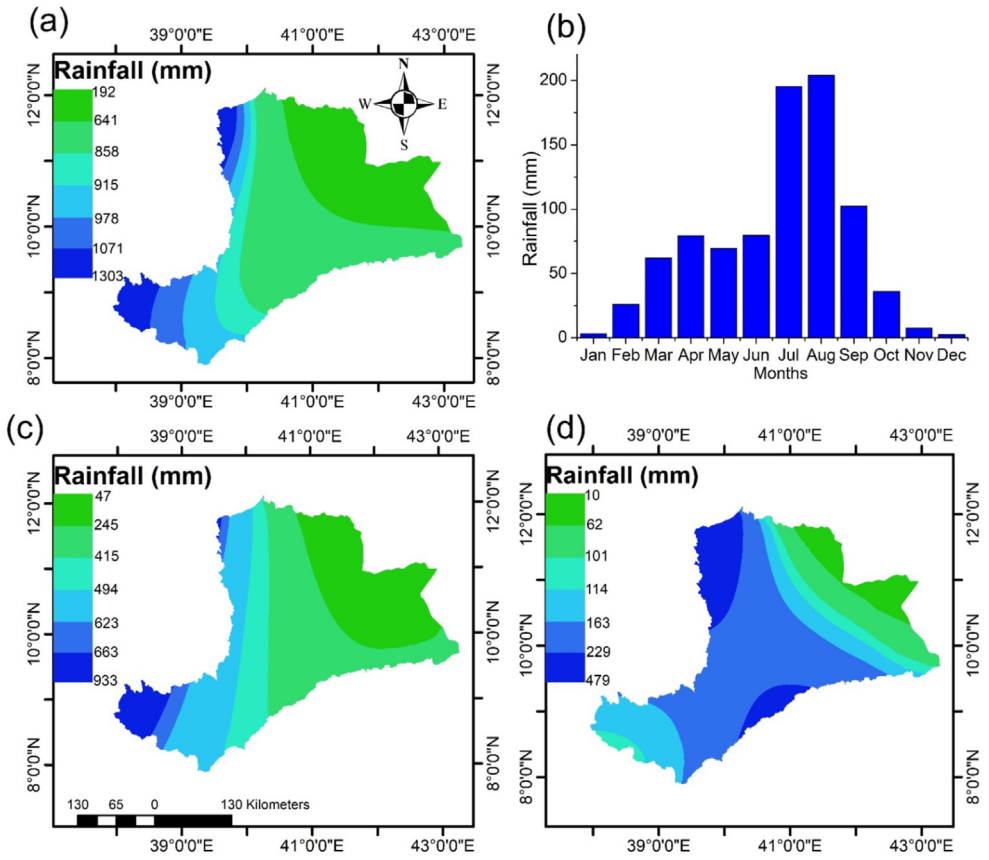

Figure 2. Spatial average annual and seasonal rainfall distribution of Awash river basin from (1986–2016): a) annual rainfall, b) average monthly rainfall, c) major rainy season rainfall, d) minor rainy season rainfall.

$$CV = \left(\frac{S}{\bar{y}}\right)*100 \tag{2}$$

where, Y_i is the observed time series rainfall of a particular time, $\bar{y}$ is the average rainfall from 1986 to 2016, and S is standard deviation. The degree of variability of rainfall was categorized as low when CV < 20%, moderate when 20% < CV < 30%, high when 30% < CV < 40%, very high when 40% < CV < %70, and extremely high when CV > 70 (Hare, 2003; Asfaw et al., 2018).

3.3. Interpolation of rainfall

The Inverse Distance Weighting (IDW) interpolation method using ArcGIS was used for rainfall interpolation as it provides relatively small root mean square and mean errors. IDW is interpolation is also recommended for uneven and sparse station distribution (Apaydin et al., 2004; Goovaerts, 2010). The prediction at an unsampled point is inversely proportional to the distance to the measurement points.

Inverse distance weighting equation

$$z(\mathbf{X}) = \sum_i w_i z_i \Big/ \sum_i w_i \qquad w_i = 1/d_i^2 \tag{3}$$

where, d_i is the distance between stations with unsampled point to that of nearby station having data.

Z_i is recorded data in the nearby station, and z(**x**) is station with unsampled data.

The power parameter (default power value of two) controls the local effect and how the local influence weakens with distance. The prediction becomes the average of all measured values if the power values equals to zero. Moreover, the immediate few nearby points will have influence on the prediction if the power value is very high. With the power value of two the interpolation is also known as IDW.

3.4. Correlation coefficient

The rainfall pattern correlation analysis with sea surface temperature anomaly, local temperature and elevation was computed by r studio software using Pearson correlation coefficient (r) as defined by (Spiegel, 1998; Pearson, 1920). A two-tailed, 5% significance level was used for this study, assuming that both variables are normally distributed. Suppose that the two correlating variables are y (rainfall) and T (temperature), both owing n values Y_1, Y_2, Y_3.... and T_1, T_2, T_3…, correspondingly, and then r is defined as follows:

$$r = \frac{\sum(y_i - \overline{X})(T_i - \overline{T})}{\sqrt{\sum(y_i - \bar{y})^2 \sum(T_i - \overline{T})^2}} \tag{4}$$

where the summation continues along all n probable values of Y and T in this sample. Let, $\overline{Y}$ and $\overline{T}$ are the average of Y and T in this sample. Correlation coefficient (r) varies between -1 ≤ r ≤ 1. When r close to -1 indicates that as rainfall increase, there is an exact predictable decrease in temperature and in the other hand when r close to 1 indicates that as rainfall increase, there is an exact predictable increase in temperature. However, when r close to 0 indicates that as rainfall increase or decrease, temperature can't be predicted.

3.5. Mann-Kendall trend analyses

Mann-Kendall (MK) that is non-parametric test was used for trend analysis of both seasonal and annual rainfall and temperature using r

studio software. The MK test has been performed in many studies across the globe and it detects the presence of monotonic (increasing or decreasing) trends and whether the trend is statistically significant or not (Spearman, 1904; Lehmann, 1975; Suhaila and Yusop, 2018; Onyutha, 2021). The MK test statistic 'S' is calculated based on Mann (1945); Kendall (1975); Asfaw et al., 2018 using the formula:

$$S = \sum_{i=1}^{n-1} \sum_{j=i+1}^{n} sgn\left(y_j - y_i\right) \tag{5}$$

Trend test is applied to a time series Y_i that is ranked from i = 1, 2…n-1 and Y_j, which is ranked from j = i+1, 2…. n. Each of the data point Y_i is considered as a reference point which is compared with the remaining of the data point's Y_j in such a way that:

$$Sgn\left(y_j - y_i\right) = \begin{cases} +1 \text{ if } \left(y_j - y_i\right) > 0 \\ 0 \text{ if } \left(y_j - y_i\right) = 0 \\ -1 \text{ if } \left(y_j - y_i\right) < 0 \end{cases} \tag{6}$$

where Yi and Yj are the yearly or seasonal values in years i and j (j > i) correspondingly. MK has been recognized that when the number of observations is more than 10 (n ≥ 10), the statistic 'S' is nearly normally distributed with the average and variance becomes 0 (Kendall, 1975). In this case, the variance (Var (S) or (σ^2)) is considered as:

$$Var(S) = \frac{1}{18}\left[n(n-1)(2n+5) - \sum_{t=1}^{m} t_i(t_i-1)(2t_i+5)\right] \tag{7}$$

where n is the number of observation, and m is the number of tied groups (a set of t_i sample time series data owning the same values). The standardized statistics test Z is given as below:

$$Z = \begin{cases} \dfrac{S-1}{[Var(S)]^{1/2}} \text{ if } S > 0 \\ 0 \quad \text{if } S = 0 \\ \dfrac{S+1}{[Var(S)]^{1/2}} \text{ if } S < 0 \end{cases} \tag{8}$$

where Z indicates a normal distribution, a +ve Z and a -ve Z show increasing and decreasing trend for the series, respectively. Accordingly, the null hypothesis (H_0) indicates that the observed data (y_1,. ., y_n) comprise of a sample of n random variables that are independent as well as identically distributed. For the alternative hypothesis (H_1) that is a two-sided test the distributions of y_i and y_j are not identical for all i, j ≤ n with i≠ j. For H_0 (no trend) is considered if Z < Zα/2, whereas rejected (H_1) if Z > Zα/2, where α is the significance level and Zα/2 the standard normal distribution for α/2. For this study the Mk test with 95% confidence level (α = 0.05) were considered with $Z_{\alpha/2} = 1.645$). In the MK test, the negative value of slope indicates a decreasing trend, while the positive value of slope illustrates an increasing trend. The magnitude of the trend itself can't be estimated by the MK test. Hence, Sen's slope estimation test calculates both the slope and intercept. The magnitude of the trend is estimated by Theil (1950); Sen (1968) slope estimator methods. The slope (β_{ij}) of all data pairs is calculated as (Sen, 1968). Overall, β_{ij} between any two values of a time series y will be projected from:

$$\beta_{ij} = Median\left(\frac{y_j - y_i}{j - i}\right) \tag{9}$$

for k = 1, 2, ..., N, which y_j and y_i are considered as dataset values at time j and i (j > i) correspondingly, and N is the number of all pairs y_j and y_i. The calculated pairwise slopes are ordered from smallest to largest and relabeled as β(1), β(2)… β(n). The median slope (Q) of these N all paired values is denoted as Sen's estimator of slope that is calculated as Qmed? $\beta_{([N+1]/2)}$ if N becomes odd, and it is taken as Qmed? ($\beta_{([N/2])} + \beta_{([N+2])/2}$)/2 if N becomes even. A positive value of β shows an increasing trend and a negative value of β provides a decreasing trend.

3.6. Tests for change-point detection

Non-parametric ranking tests, namely Pettit's and the VNR, and parametric tests, namely the BR and the SNH were performed for change-point detection tests of rainfall and temperature on annual, seasonal, and monthly basis. A non-parametric approach is useful when assumptions are not made about the data distribution, and can better deal with data containing outliers. It is also less sensitive to sample size (Whitley and Ball, 2002). The opposite is true for the parametric test. For all change-point detection tests if ρ-value is smaller compared to the specific significance level (in this case 0.05), the H_0 i. e, that there is no change-point is rejected.

The Pettit's test is the most commonly used test and calculated in the same way as MK test, and it assumed to have a normal distribution thus allowing the z-value to be calculated (Zarenistanak et al., 2014; Jaiswal et al., 2015). It identifies a significant change in the average of a time series when the exact time of the change is unknown by considering a series of dataset $Y_1, Y_2,\ldots, Y_n$, that has a change-point at "n" such that Y_1, Y_2,.., Y_n has a distribution function $F_1(y)$ that is dissimilar from the distribution function $F_2(y)$ of the subsequent portion of the sequence y_{n-1}, y_{n-2}, y_{n-3} …, y_n. Pettit test statistics $S_{n-1,\ n}$ can be described as follows: From MK test statistic $S_{n-1,\ n}$ Eqs. (5) and (6), the Pettit test statistic (K) and the related confidence level (α) for the sample length (n) can be defined as:

$$K = Max|S_{n-1,\ n}| = \max\left(K_+, K_-\right) \tag{10}$$

$$\alpha = \exp\left(\frac{-K}{n^2 + n^3}\right) \tag{11}$$

when α is less as compared to confidence level (0.95), H_0 is rejected. The estimated significance probability (P) for a change in point is described as given below:

$$P = 1\text{-}\alpha \tag{12}$$

when significant change-point exists, the series is divided at the location of the change-point into two subseries. Moreover, the K can also be associated with standard values at various confidence levels for detection of change-point in a series.

The VNR test is a bit connected to first-order sequential correlation coefficient (r) and has been explained by (Buishand, 1982; Javari, 2016; Suhaila and Yusop, 2018). The VNR test for a sequence of observation data y_1, y_2, $y_3\ldots y_n$ can be designated as:

$$N = \frac{\sum_{i=1}^{n-1}\left(y_i - y_{i-1}\right)^2}{\sum_{i=1}^{n}\left(y_i - \overline{y}\right)^2} \tag{13}$$

where y_i is the i^{th} data values, based on this test the expected value E(N) = 2 under the null hypothesis will have a constant mean if the series is homogenous. In the other hand, when the dataset has a shift, then the N value must be lower than 2, else it indicate that the dataset has rapid deviation in the mean that show the changing-point critical values of N. The null hypothesis for the VNR test is that the data are independent and identically distributed random values, while the alternative hypothesis is that the values in the series are not randomly distributed. The VNR test is defined as the ratio between the mean square successive (year-to-year) difference and the variance of the data. If the data are homogeneous, it is expected that the VNR test statistic = 2. Otherwise, the value must be <2, implying that the sample mean rapidly varies. Thus, the critical values from the VNR test at 5% confidence levels can be used to identify change-points in a non-homogeneous series (Table 2 of Jaiswal et al., 2015).

The Buishand's test (1982) parametric approach rely on the assumption of normal distribution. It is sensitive to outliers and sample size (Gali, 2015). The adjusted partial sum (S_k), which is the cumulative variation from average for k^{th} observation dataset of a sequence y_1, y_2, y_3 ….y_k…. y_n with average ($\bar{y}$) will be calculated using:

$$S_k = \sum_{i=1}^{k} (y_i - \bar{y}) \quad (14)$$

A series can be uniform when there is no change-point if $S_k \cong 0$, as in random series, the variation from average will be distributed on both sides of the average of the series.

A significance of shift (a break-point from average) can be assessed by calculating rescales adjusted range (R) as:

$$R = \frac{\mathrm{Max}(S_k) - \mathrm{Min}(S_k)}{\bar{y}} \quad (15)$$

The value of $R/\sqrt{n}$ is compared with critical values to show detection of probable change-point.

The parametric SNH test and its statistic (T_k) is accustomed to associate the average of first n observations with the average of the remaining (n-k) observations with n dataset points (Ros et al., 2015; Jaiswal et al., 2015; Suhaila and Yusop, 2018).

$$T_k = kZ_1^2 + (n-k)Z_2^2 \quad (16)$$

Z_1 and Z_2 can be computed as:

$$Z_1 = \frac{1}{k}\sum_{i=1}^{k} \frac{(y_i - \bar{y})}{\sigma x} \quad (17)$$

$$Z_2 = \frac{1}{n-k}\sum_{i=k+1}^{n} \frac{(y_i - \bar{y})}{\sigma x} \quad (18)$$

where, $\bar{x}$ represents the mean of the series, σx assigns the standard deviation of series. K represents the year, and taken as a break when the value of T_k attains the maximum value. The test statistic should be greater than the critical value so as to reject the null hypothesis and consider the alternative. The critical values of Pettit (K), VNR (N), Buishand ($R/\sqrt{n}$) and SNH(T_k) at 1 and 5 % confidence levels for the varies tests were presented in (Buishand, 1982; Ros et al., 2015; Jaiswal et al., 2015).

The null hypothesis of BR test is that the annual values of the testing variable are independent and identically distributed, and the alternative hypothesis is that a step-wise shift in the mean is present. In this test an adjusted partial sum is calculated, comprising the cumulative variation of each sample from the average. Then, the range of the adjusted partial sum for all of the samples is used to detect the change-point, based on the critical values given by Buishand (1982).

The same null and alternate hypotheses apply for the SNH test as for the BR test. In addition, in the SNH test the mean of a subset of the observations is combined with the mean of the remaining observations to form the test statistic. Then, the sample at which the test statistic attains a maximum value can be a change-point, based on the total number of observations (Table 2 of Jaiswal et al., 2015). In Pettit's test, the same null hypothesis and alternative hypotheses are used as in the SNH and BR tests. However, Pettit's test is based on the ranks of elements in a series, and thus the sums of the difference between observations on both sides of a chosen pivot are calculated. Then, the maximum value of this sum obtained for all pivots is used to identify the change-point, based on the number of observation and chosen confidence level (Javari, 2016).

The Pettit's, BR, and SNH change-point detection tests reveal the exact year of the change-point, but the VNR test cannot do so: it only determines the existence of a change-point. Pettit's and BR tests tend to detect a change-point years in the middle of the series, whereas the SNH test is more sensitive in detecting a change-point years near the beginning and end of the time-series because of its different hypothesis and method of critical value attainment (Ros et al., 2015). Thus, using multiple change-point tests will help to detect all possible change-point years with smaller error and higher accuracy than one or two change-point tests (Reeves et al., 2007). The details of these change-point detection tests, their statistical formulas, and the confidence level critical values are presented in Javari (2016); Jaiswal et al. (2015) and Zarenistanak et al. (2014). A series is considered to have a change-point year if more than two tests reject the null hypothesis, or when two tests report the same change-point year (Jaiswal et al., 2015). Change-point detection test was computed using XLSTAT software and excel spreadsheet.

4. Results and discussion

4.1. Trend analysis and coefficients of variation (CV)

Trend and change-point analysis of average temperature and rainfall were carried out for the entire ARB, using the entire basin as one series and using each station in the basin individually, on annual and seasonal basis from 1986-2016. Additionally, change-point analysis and trends of monthly temperature and rainfall were examined for the entire basin as one series.

4.1.1. The entire ARB average temperature and rainfall

The MK trend test was applied on average temperature and rainfall of the entire ARB. The MK test indicated a significant increasing trend in temperature on annual, seasonal and monthly basis, except for December, which is the coldest month in Ethiopia (Table 1). The annual rainfall decreased non-significantly, whereas the major rainy season rainfall increase non-significantly. At the same time, the mRS rainfall decreased significantly. The Sen's slope rate of mean annual rainfall decrease was -1.29 mm/y, while the rate of MRS rainfall increase was 0.004 mm/y (Table 1). On a monthly basis, February indicated a significant declining trend in rainfall. A non-significant declining trend in rainfall was observed in March, April, June, and September, whereas May, July, and August showed a non-significant increasing trend in rainfall.

The annually and MRS rainfall CV were 22.5% and 32.1%, implying moderate and high variability of rainfall, respectively (Table 1). Likewise, the CV of the mRS was 57.2%, implying that there was a very high variability in rainfall. At the same time, the monthly CV showed less variability in August (10.4%), while it showed moderate variability in June (24.6%). During the mRS, there was extremely high variability in

Table 1. MK test and CV analysis of entire ARB average rainfall and temperature plus AMO SST.

Months, Season	Rainfall (mm)			Mean Temp (^{O}C)		AMO SST (^{O}C)	
	CV %	p-value	Sen's slope	p-value	Sen's slope	p-value	Sen's slope
Jan	76.8	0.919	-0.003	**0.001**	0.035	**0.0001**	0.016
Feb	98.8	**0.013**	-1.140	**0.001**	0.046	**0.0001**	0.014
Mar	46.5	0.518	-0.531	**0.003**	0.045	**0.001**	0.012
Apr	38.4	0.062	-1.203	**0.001**	0.061	**0.001**	0.012
May	44.0	0.185	0.906	**0.001**	0.051	**0.001**	0.013
Jun	24.6	0.415	-0.320	**0.0001**	0.037	**0.011**	0.012
Jul	16.2	0.153	0.993	**0.0001**	0.034	**0.002**	0.016
Aug	10.4	0.518	0.352	**0.002**	0.022	**0.000**	0.018
Sep	21.3	0.352	-0.285	**0.0001**	0.038	**0.0001**	0.019
Oct	74.9	0.415	0.403	**0.0001**	0.036	**0.0001**	0.021
Nov	99.3	**0.025**	0.155	**0.001**	0.053	**0.0001**	0.017
Dec	98.8	0.066	-0.049	0.324	0.012	**0.0002**	0.015
MRS	32.1	0.919	0.004	**0.0001**	0.032	**0.0003**	0.016
mRS	57.2	**0.049**	-0.56	**0.0001**	0.051	**0.000**	0.013
Annual	22.5	0.659	-1.29	**0.0001**	0.040	**0.0001**	0.015

P-value in bold indicates a significant increasing trend.

February, with a CV of 98.8%. The remaining months of the mRS showed very high variability, indicating the high uncertainty of mRS rainfall in a given year.

4.1.2. Average temperature and rainfall of each station in the ARB

Trend analysis of average temperature and rainfall were performed not only for the entire basin, but also for each of the meteorological stations in the basin. A significant increasing trend in annual and seasonal temperature were found at all of the meteorological stations, whereas Mojo, Debre Zeit, Kulumsa and Harbu stations showed non-significant temperature increase. A significant decreasing trend in annual rainfall was detected at Asgori, Gewane, Merssa, and Assaita meteorological stations, but most of the meteorological stations indicated a non-significant decreasing trend (Figure 3). Rainfall during the MRS showed a significant decreasing trend at the Gewane and Asgori meteorological stations. The other ten meteorological stations revealed a non-significant declining trend in rainfall, whereas the remaining 17 stations showed a non-significant increasing trend in rainfall (Figure 3). In the mRS, a significant decreasing trend of rainfall was observed at eight meteorological stations (Dubity, Gewane, Erer, Bati, Merssa, Asgori, Awash 7 Kilo and Assaita), which are all located in the downstream part of the ARB. The remaining meteorological stations indicated a non-significant decreasing trend, with the exception of Lefessa and Mojo meteorological stations.

The mean annual and seasonal spatial variability of rainfall from each station was interpolated over the basin as indicated in (Figure 4). In the annual and MRS, high and very high variability of rainfall were noticed in the downstream part of the ARB, while less variability was observed in the upstream part of ARB. Similarly, extremely high variability of rainfall was noticed in the downstream area of the ARB during the mRS, whereas moderate variability was observed in the upstream part of the ARB. High rainfall variability was observed in the mRS than in the annual and MRS.

A significant increase in temperature and rainfall variability has been reported in different parts of Ethiopia (Hayelom et al., 2017; Tamiru et al., 2015), which is in line with our results. However, the significant decline of rainfall in the mRS and especially in the lowland part of the

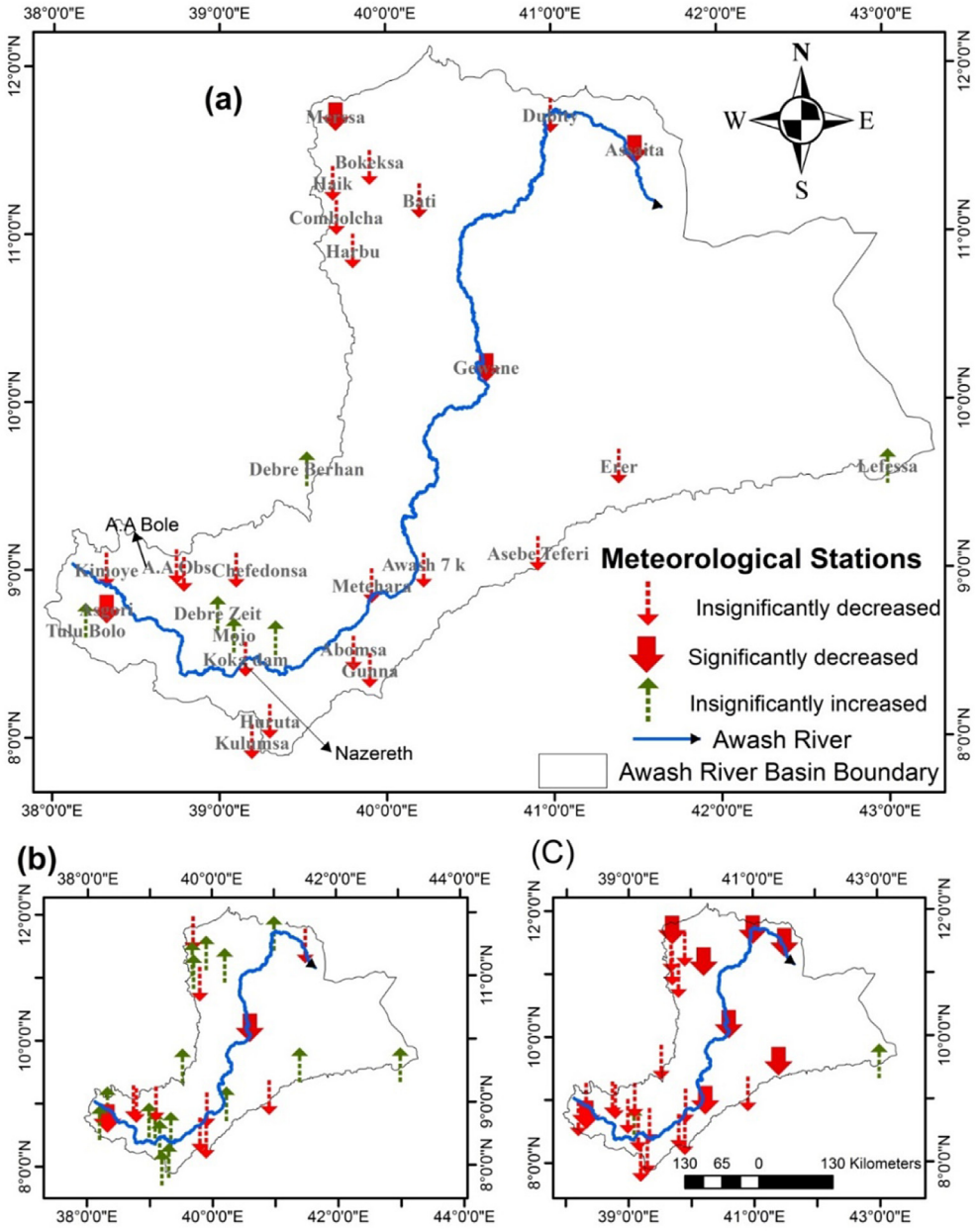

Figure 3. Station-wise annual and seasonal trends of rainfall in Awash river basin from (1986–2016): a) annual, b) major rainy season, c) minor rainy season.

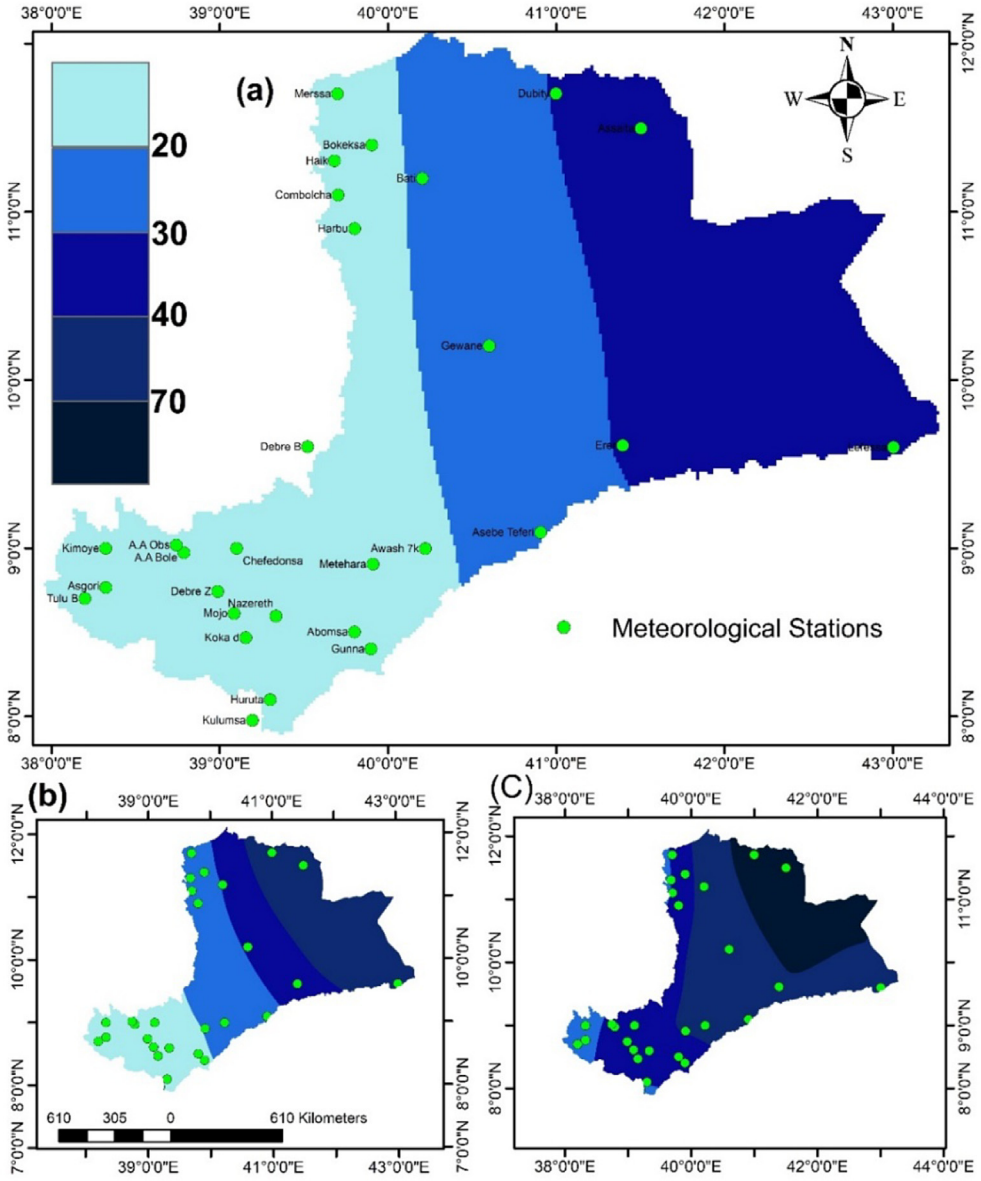

Figure 4. Spatial variability of annual and seasonal rainfall in Awash river basin from (1986–2016): a) annual, b) major rainy season c) minor rainy season.

ARB was a novel finding in our case. A similar finding that mRS rainfall is more variable than the MRS rainfall has been reported in the northern part of Ethiopia (Hayelom et al., 2017).

Based on gridded reanalysis rainfall data, Mulugeta et al. (2019) detected a significant decreasing trend of MRS rainfall, whereas the annual, mRS and dry rainy season rainfall showed no trend in the entire ARB in which most of the findings were not similar with our result. The gridded data uncertainty relating with topography, resolution and different periods used for the MK test might cause the disagreement. On the other hand, a non-significant increasing trend of MRS rainfall was detected in the entire ARB based on 12 stations, whereas the annual and mRS rainfall indicated the contrary (Bekele et al., 2017). Our result is also in line with the findings of Bekele et al. (2017), except that the mRS rainfall decreased significantly in our case. Because of the less number of stations (i.e. 3) that Bekele et al. (2017) used from the downstream part of the basin, it was difficult to compare the significant decreasing trend of mRS rainfall that it was occurred in the downstream part of the basin in our finding. Over the entire ARB, a significant decreasing trend of annual rainfall was detected in 5 out of 28 stations, whereas two stations indicated the contrary and the remaining non-significant trend (Tadese et al., 2019). Commonly used stations with our study were 11 out of 28, but the periods used for the MK test were different. Tadese et al. (2019) also used less number of station from the downstream part of the basin. Four stations were used from the downstream part of the basin such as Mersa, Kombolcha, Adaiytu and Mile, 2 of them showed significant decreasing trend of mRS rainfall, while the remaining 2 depicted non-significant decreasing trend that resembles with our finding.

The rainfall in mRS showed higher variability than in the MRS and annual that matches with our result (Tadese et al., 2019). Similarly, the MRS and mRS rainfalls were showed non-significant trend. Gedefaw et al. (2018) also carried out MK trend analysis of rainfall and temperature in the ARB. However, the location information of all the stations in this study is wrong. Even if we use the correct locations of these stations according to the Ethiopian Meteorological Agency website, some of them are still far from the ARB (see http://www.ethiomet.gov.et/stations/regional_information for more information). Therefore, we only used their results from Gewane and Bui stations for comparison with our study. Gedefaw et al. (2018) detected a significant increasing trend of average annual temperature in Gewane and Bui stations of ARB that is similar with our finding. Gewane station found to have a significant

increasing trend of annual rainfall, whereas Bui station demonstrated a non-significant decreasing trend. We commonly used Gewane station only but our finding was contrary to Gedefaw et al. (2018) that will be due to the different period data used for the MK test that they used from 1993-2006, while we used from 1986-2016. Likewise, Shawul and Chakma (2020) found a significant increasing trend of maximum temperature and a non-significant trend of annual rainfall in the upper ARB that was parallel with our finding. Generally, except the study based on the gridded data, most of the previous studies based on the observed data showed a good agreement with our finding.

4.2. Change-point detection tests of temperature and rainfall

4.2.1. The entire ARB average temperature and rainfall

The Pettit and VNR, BR, and SNH change-point detection tests were performed to detect the presence of shifts in the annual, seasonal and monthly series of temperature and rainfall data during the period 1986–2016 (Table 2 and Table 3). Analysis of the annual and MRS temperature indicated that there was a change-point in 2001. In this case, the mean annual temperature increased from 20.6 °C to 21.2 °C, with an increase of 0.6 °C after the change-point. Similarly, the MRS temperature increased by 0.52 °C after the change-point (Figure 5). According to the BR and SNH tests, the change-point of the mRS temperature was detected in 1997, whereas Pettit's test indicated that the change-point in 2001 (Table 3 and Figure 5). The mRS temperature shifted three years earlier than annual and MRS indicating that mRS months are highly sensitive to global warming. The change-point of average monthly temperature was detected in all months except for December, yet the change-point year varied based on the type of test. The highest average temperature increase after the change-point was 1.1 °C in April, May, and November, while the lowest increase was 0.5 °C in July, August, and September (Table 3). The MK trend test was applied to the temperature data before and after the change-point, and was found to significantly increase both before and after the change-point.

There was no significant trend and change-point of temperature in the coldest month December, which indicated that it is relative insensitive to global warming. The mean temperature of April, May, and June shifted three years earlier than others did indicting that these three months were highly sensitive to global warming. This in turn will potentially affect the agricultural productivity in the ARB.

There were no change-points identified for rainfall either yearly or during the MRS. However, the mRS change-point for rainfall was detected in 1998 based on the BR and SNH tests, with a mean rainfall decrease from 267.6 mm to 215.1 mm (Figure 5 and Table 2). Furthermore, the Awash River basin's average monthly rainfall change-point was detected in February 2000 using the Pettit and VNR and BR tests. The VNR and BR tests showed a change-point in April 2000, but as the VNR test does not identify a change-point year, it could not be inferred that April was the rainfall change-point month (Table 2). Pettit's test detected comparatively fewer change-points for rainfall, while the BR and VNR tests detected more change-points. The rainfall trend before and after the change-points were assessed; thus the annual and seasonal rainfall trends were non-significant. Analysis of annual and MRS temperature indicated that there was a change-point in 2001, whereas the annual and MRS rainfall showed no change-point existed. The mRS change-point of rainfall was one year later than the change-point of temperature (Figure 5).

4.2.2. Average temperature and rainfall of each station in the ARB

In addition to the entire ARB's average rainfall analysis, station-wise change-point identification tests of annual and seasonal average temperature as well as rainfall were performed. The annual temperature change-point were confirmed in 19 meteorological stations out of the 29 as indicated in Figure 6, a. The highest mean annual temperature shift occurred in Assaita station in 1997 that increased from 29.2 °C to 31.7 °C, with an increase of 2.5 °C after the change-point. Following Assaita station, the highest mean annual temperature shift detected in Gewane station in 2001, Combolecha station in 1997, Tulu Bolo station in 1997, and Asebe Teferi station in 2001 with the corresponding mean annual temperature increase of 2.3 °C, 2.2 °C, 1.4 °C, and 1.3 °C after the change-point. On the other hand, the lowest mean annual temperature shift occurred at Bokeksa station in 2001 that it increased from 21.6 °C to 21.9°. Excluding Bokeksa station, all the meteorological stations that is 18 out of 29 confirmed the mean temperature change-point of MRS similar to that the annual (Figure 6b). The highest MRS mean temperature shift occurred in Assaita and Combolecha in 1997 that the mean increased from 31.4 °C to 34.0° and 17.8 °C to 20.4°, respectively, with an increase of 2.6 °C after the change-point. Whereas, the lowest mean MRS temperature increase after the change-point were 0.4 °C in Metehara, and 0.5 °C in Awash 7 kilo, A.A Obs, and Debre Berhan stations. After the change-point, the mean MRS temperature increase in Gewane, Tulu Bolo, and Asebe Teferi were 2 °C, 1.8 °C and 1.3 °C, respectively.

Meteorological stations of 20 out of 29 confirmed the mRS mean temperature change-point as shown in Figure 7 that includes stations of Kokadam and Merssa but not Debre Berhan. In most of the stations the mRS temperature change-point were detected in 1997/98, while the

Table 2. Entire basin changing point detection of average annual, seasonal and monthly temperature (1986–2016).

Months, Seasons	Pettit's test			VNR	BR test			SNH test		
	Year of shift	Temp		P-value	Year of shift	Temp		Year of shift	Temp	
		Pre	Post			Pre	Post		Pre	Post
Jan	2002	18.72	19.44	Yes	2002	18.72	19.44	2002	18.72	19.44
Feb	2002	19.84	20.68	Yes	2002	19.84	20.68	2002	19.84	20.68
Mar	1997	20.97	21.64	Yes	2001	21.13	21.74	2001	21.13	21.74
Apr	1997	21.36	22.42	Yes	1997	21.36	22.42	1997	21.36	22.42
May	1998	22.09	23.13	Yes	1997	22.04	23.11	1997	22.04	23.11
Jun	1997	22.61	23.25	Yes	1999	22.66	23.28	1997	22.61	23.25
Jul	2000	21.46	22.01	No	2000	21.46	22.01	2000	21.46	22.01
Aug	2000	20.99	21.39	Yes	2000	20.99	21.39	2000	20.99	21.39
Sep	2001	20.97	21.52	Yes	1997	20.78	21.45	1997	20.78	21.45
Oct	2000	19.98	20.57	Yes	2000	19.98	20.57	2000	19.98	20.57
Nov	2001	18.89	19.96	Yes	2001	18.89	19.96	2001	18.89	19.96
Dec	No	18.54		0.86	No	18.54		No	18.54	
Major	2001	21.54	22.06	Yes	2001	21.54	22.06	2001	21.54	22.06
Minor	2001	21.20	22.00	Yes	1997	21.07	21.92	1997	21.07	21.92
Annual	2001	20.58	21.24	Yes	2001	20.58	21.24	2001	20.58	21.24

Table 3. Entire basin changing point detection of average annual, seasonal and monthly rainfall (1986–2016).

Months, Seasons	Pettit's test			VNR	BR test			SNH test		
	Year of shift	Mean rainfall		P-value	Year of shift	Mean rainfall		Year of shift	Mean rainfall	
		Pre	Post			Pre	Post		Pre	Post
Jan	No	2.37		No	No	2.37		No	2.37	
Feb	2000	54.53	15.9	Yes	2000	54.53	15.9	No	25.94	
Mar	No	62.24		No	No	62.24		No	62.24	
Apr	No	79.36		Yes	1998	79.36	72.17	No	79.36	
May	No	69.8		No	No	69.8		No	69.8	
Jun	No	78.83		No	No	78.83		No	78.83	
Jul	No	198.74		No	No	198.74		2001	195.74	189.2
Aug	No	204.98		No	No	204.98		No	204.98	
Sep	No	101.95		No	No	101.95		No	101.95	
Oct	No	36.52		Yes	No	36.52		No	36.52	
Nov	No	7.89		No	No	7.89		No	7.89	
Dec	No	2.18		No	No	2.18		No	2.18	
Major	No	582.74		No	No	582.74		No	582.74	
Minor	No	235.41		No	1998	267.6	215.1	1998	267.6	215.1
Annual	No	866.83		No	No	866.83		No	866.83	

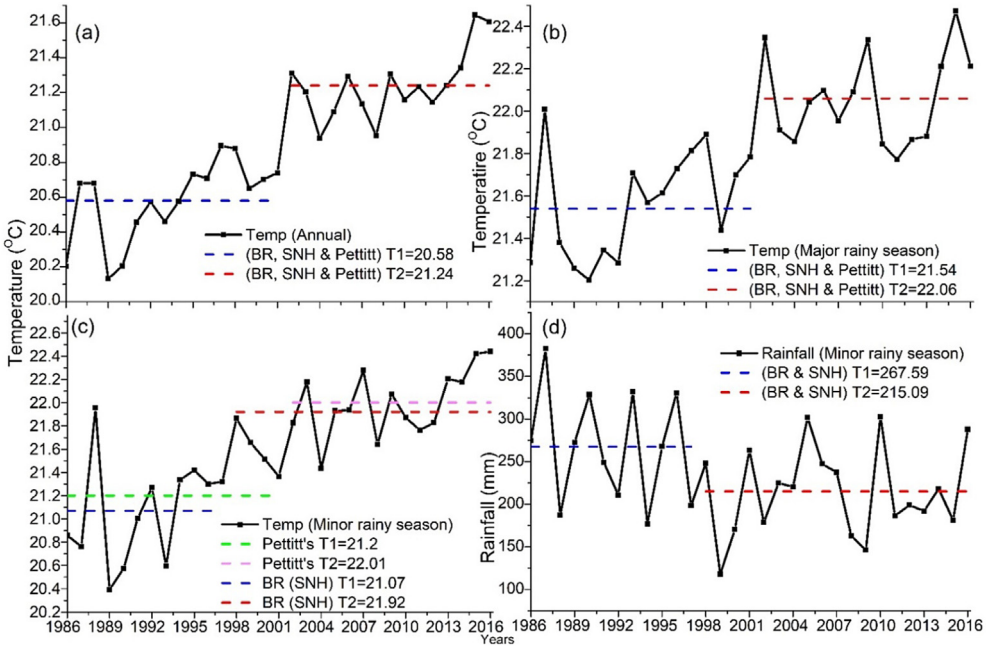

Figure 5. Awash River basin average rainfall and temperature change-point using BR, SNH and Pettit's tests, T1 is the average temperature or rainfall value before the changing point and T2 is average value after the changing point: a) annual temperature, b) MRS temperature, c) mRS temperature, and d) mRS rainfall.

annual and MRS change-point were in 2000/2001. The highest mean mRS temperature shift detected in Gewane station that it increased from 27.9 °C to 30.8 °C with the mean increase of 2.9 °C after the change in point. After the change-point, the mRS mean temperature of Assaita, Combolecha, Tulu Bolo, increased by 2.7 °C, 2.6 °C, 2.4 °C, respectively.

In general, 10 out of the 29 meteorological stations indicated that a change-point of rainfall occurred in the annual and/or seasonal series (Figure 8). At the remaining meteorological stations there was either a change-point in only one or two types of tests in different years, or no change-point at all. Most of the change-points were detected in the downstream part of the ARB.

In most of the observations the major change-point years were 1997/98 and 2001/02, though there were variations from one test to another. The change-point of rainfall for the mRS occurred in 1997/98, whereas for the MRS and annual rainfall the change-point was typically in 2001/2002. At Gunna station, the highest MRS average rainfall shift was detected in 2002, using all change-point detection tests. Before the change-point in 2002, the average JJAS rainfall value was 884 mm, whereas after the change-point the mean JJAS rainfall decreased to 669 mm. The next highest average-rainfall shift was detected at Erer station in 1998, using all change-point detection tests for the mRS. The mean rainfall before the change-point was 401 mm and 240 mm after (Figure 8). Station-wise trend analysis was performed before and after the change-points, and there were no significant trends detected.

Similar to our result a study in Malaysia showed the change-point of rainfall and temperature in 1997/98 and 2001/02. The change-point in Malaysia were related to ENSO and La Niña events, or to urbanization (Suhaila and Yusop, 2018). The change-point of rainfall and temperature caused by ENSO was also detected in 2001/02 in India and Nigeria (Dibal et al., 2017; Bisai et al., 2014). Drastic changes in land use-land cover,

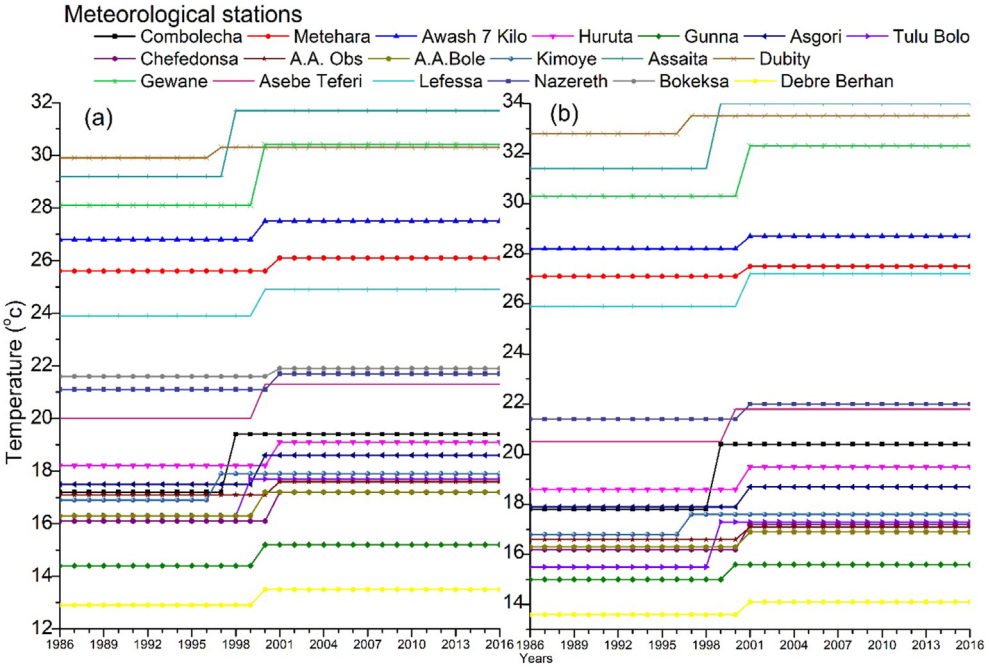

Figure 6. Station based average temperature change-point using (BR, SNH and Pettit) tests and the temperature shift plot before and after the change-point: a) annual, b) major rainy season.

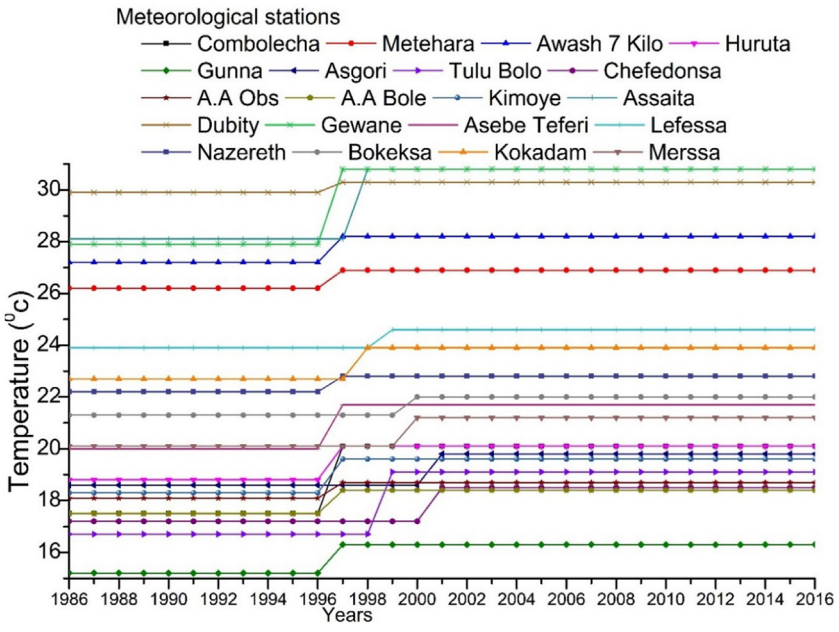

Figure 7. Station based average temperature change-point using (BR, SNH and Pettit) tests and the temperature shift plot before and after the change-point in minor rainy season.

from forest/grassland to agricultural land, have occurred in the ARB in association with increasing population and that would have contributed to the shifts of rainfall and temperature (Getahun and HAJ, 2015). The change-point of rainfall and temperature in a given region would also be due to topographical variation, relocation of meteorological stations, and urbanization (Sahin and Cigizoglu, 2010).

4.3. The influence of elevation on the Awash River basin's rainfall

The elevation of ARB meteorological stations was correlated with their rainfall datasets. The correlations of station elevation to station rainfall for the annual, MRS (JJAS) and mRS (FMAM) were 0.79, 0.81 and 0.52, respectively (Figure 9). The meteorological stations at high elevations showed higher rainfall relative to those at low elevations, and the rainfall variation among meteorological stations was strongly related to the differences in elevation. As a result, it was found that the rainfall magnitude decreased from the upstream to the downstream (lowland) region of the ARB.

To examine the influence of elevation on the change-point, the correlation of annual and seasonal rainfalls to elevation were independently examined for 1986–2001 and 2002–2016. The correlations between annual and JJAS rainfall with elevation before and after the change-point

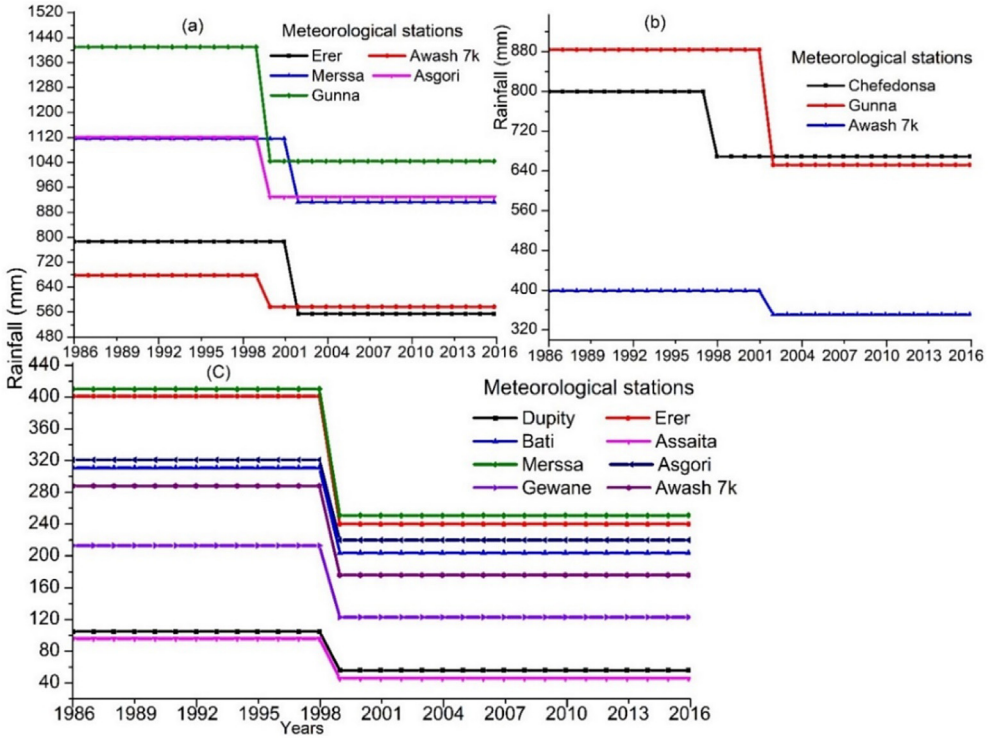

Figure 8. Station based average rainfall change-point using (BR, SNH and Pettit) tests and the rainfall shift plot before and after the change in point: a) annual, b) major rainy season, c) minor rainy season.

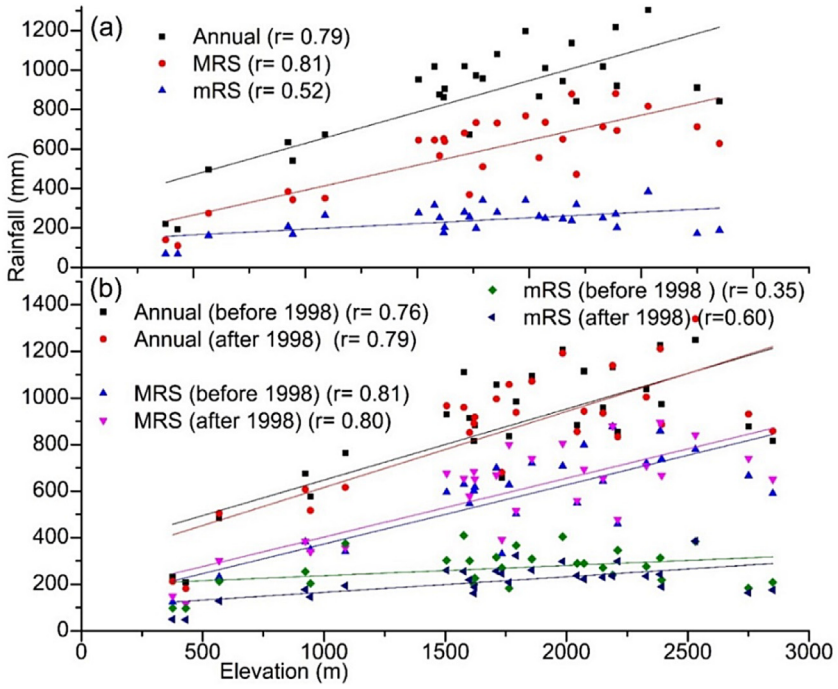

Figure 9. Awash river basin average rainfall with elevation: a) annual and seasonal rainfall correlation with elevation (1986–2016), b) annual and seasonal rainfall correlation with elevation before and after the changing point.

(2002) were almost the identical. The correlation of FMAM rainfall with elevation after the change-point in 2002 was much higher than before the change-point (Figure 9b). This indicated that the shift of rainfall might also be influenced by topography. Studies also showed that orographic rainfall is fully influenced by topography, which the effect of topography on rainfall indicated that there was a reduction of rainfall amount and shift in rainfall pattern when topography reduced implying that topography plays a great role in regional rainfall amount and spatial pattern (Enyew and Steeneveld, 2014; Ogwang et al., 2014; Ntwali et al., 2016). Summarizing that topography regulates the rainfall amount and distribution over the region.

The correlations of temperature with JJAS and FMAM rainfall were -0.26 and -0.45, respectively. The increase in temperature implies that there was a decrease in rainfall in the basin, and thus that local warming can be another cause of the significant decline of rainfall, particularly during FMAM (Zhao and Khalil, 1993; IPCC, 2007; Kuile, 2009). The contribution of JJAS and FMAM rainfalls to the annual rainfall of the basin were 58% and 42%, respectively. The mRS rainfall is a significant contributor to the total annual rainfall in the northeast, eastern and southeastern portions of Ethiopia, where a large part of the ARB is located (Fekadu, 2015). Because of the orography the mRS rainfall is limited in the east, southeast and southern parts of the country (Degefu et al., 2017).

4.4. The influence of climate variability on ARB's rainfall

4.4.1. SSTAs association with Awash River basin's rainfall

The influences of SST indexes such as the ENSO, DMI, AMO, and NTA on the change-point of ARB rainfall were also evaluated. Generally, the annual and MRS rainfall were lower than normal during the warming phase of El Niño with a correlation of -0.50 and -0.68, respectively, while an increase in rainfall was observed for the mRS with a correlation of 0.43 (Figure 10, a). This showed that during La Niña the annual and MRS rainfall increases from normal, while the mRS rainfall decrease. In this case, all of the twelve La Niña events showed an increase in rainfall during the annual and MRS, but the La Niña events in 1989, 1995 and 2011 were an exception. However, the influence of La Niña events on the mRS rainfall was highly inconsistent that only five out of 12 La Niña events showed a decrease in the mRS rainfall.

The exceptions in a few of the years, for example the increase of MRS rainfall during the minor El Niño event in 1994, could be due to the cold SST that was present in the eastern equatorial Atlantic at this time, which enhanced the northward shift of the ITCZ and monsoon troughs (Korecha and Barnston, 2007). During the MRS, most of the negative rainfall anomalies were attributable to El Niño, and the positive rainfall anomalies to La Niña. For the mRS, the opposite was true. However, the rainfall anomalies can vary substantially based on the maturity of El Niño or La Niña events. The positive anomaly of rainfall in the mRS can be partly related to the early-matured, strong El Niño events (Korecha and Barnston, 2007). Korecha and Barnston (2007) pointed out that ENSO is the most important factor governing the MRS rainfall, and that the rain-bearing mechanisms like ITCZ become weak if the El Niño event begins maturing during the late northern summer, while the contrary would occur in the case of La Niña. Thus, El Niño maturity can account for the fact that we observed that the MRS rainfall was significantly reduced in the higher El Niño events as compared to lower El Niño events.

During El Niño (warm SSTA), the horizontal wind-fields weaken the entire Indian monsoon system with a weaker Tropical Easterly Jet (TEJ) as well as weaker East African Low-Level Jet (EALLJ), which leads to the suppression of low-level moisture flux to the ARB. This causes a deficit in rainfall during the MRS (Segele and Lamb, 2005; Gleixner et al., 2016; Degefu et al., 2017). The increase of mRS rainfall with El Niño and the warming phase of the west (tropical) Indian Ocean is associated with an easterly wind anomaly, which results in enhanced moisture flux and produces wet conditions (Degefu et al., 2017; Diro et al., 2008; Marchant et al., 2007). Conversely, the cooling phase is associated with a westerly wind anomaly, which result in suppression of moisture flux and produces dry conditions. This is similar to what Diro et al. (2008) stated, i.e., that in the southwest Indian Ocean a low frequency of tropical cyclones is associated with excess rainfall in the mRS and that the opposite is also true.

In addition to ENSO, the influence of Indian and Atlantic Ocean warming and cooling on the Awash River basin's rainfall were examined. The correlation of DMI with basin rainfall was negative for the annual and seasonal series, indicating that the warming in the Indian Ocean resulted in a reduction of rainfall in the ARB. Notable, there was constant warming in the Indian Ocean during 1999–2015, which would have reduced the Awash River basin's rainfall (Figure 10).

The other large-scale climatic variability considered in this study were the AMO and the NTA from the Atlantic Ocean. The warming of a large portion of the North Atlantic Ocean and the cooling of the south is the positive phase of the AMO, and the converse is true for the negative phase of the AMO. In the case of the AMO and the NTA, a one-year lag of correlation results fitted better than a zero-year lag. As a result, the one-

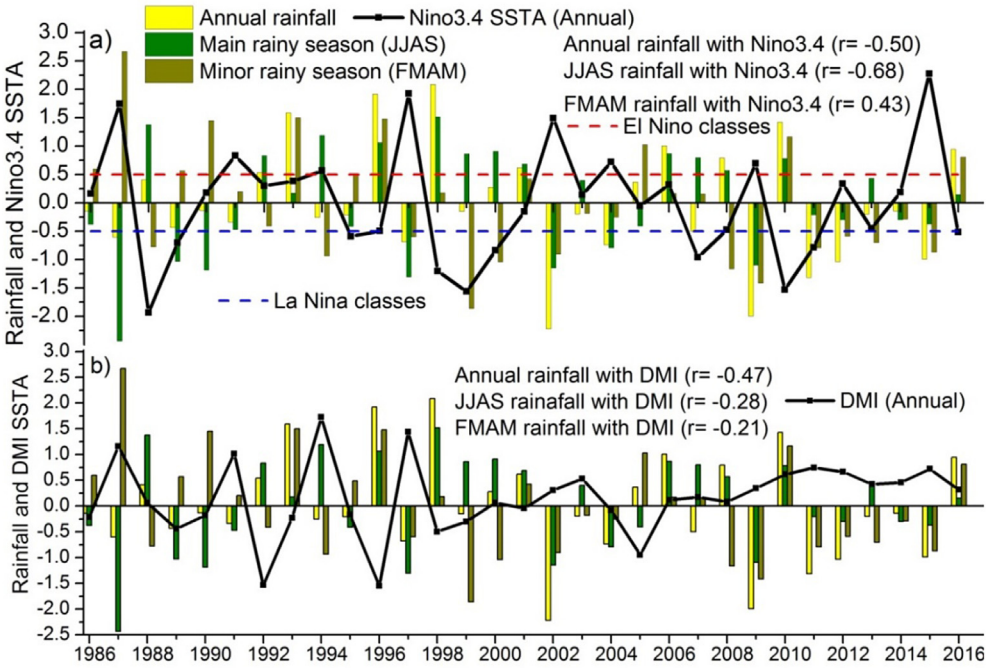

Figure 10. Basin average normalized annual and seasonal rainfall with SSTA: a) basin average rainfall correlation with Nino3.4; b) basin average rainfall correlation with DMI.

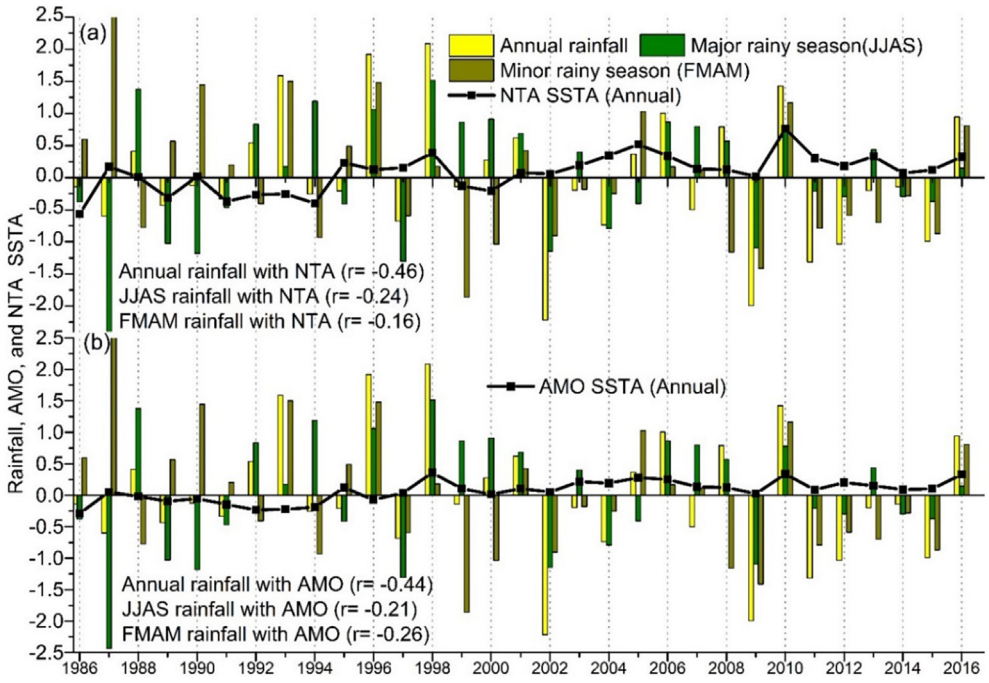

Figure 11. Basin average normalized rainfall pattern and correlation with one-year lag SSTA: a) annual and seasonal rainfall with NTA, b) annual and seasonal rainfall with AMO.

Table 4. Rainfall correlation with SST before and after change-point 1997/98 and number of El Niño/La Niña events.

SST indices	Before the changing point			No. of El Niño/La Niña		After the changing point			No. of El Niño/La Niña	
	MRS	mRS	Annual	El Ni	La Ni	MRS	mRS	Annual	El Ni	La Ni
Nino3.4	-0.71	0.29	-0.27	4	4	-0.63	0.57	-0.34	4	8
DMI	-0.42	-0.17	-0.62			0.26	-0.13	-0.26		
AMO	-0.57	0.16	-0.31			0.42	0.63	0.71		
NTA	-0.35	0.38	-0.24			0.24	0.70	-0.32		

year lag of AMO and NTA were correlated with annual and seasonal rainfall of the ARB.

The one-year lag correlations of annual rainfall with NTA and AMO were -0.46 and -0.44, respectively (Figure 11). The correlation result of AMO to the annual and seasonal rainfall was negative, which implies that a warming (positive) AMO reduces the rainfall in the ARB. Similarly, the warming of the NTA reduces rainfall in the ARB. However, the association of AMO and NTA warming with reduction of rainfall in the ARB was not true for some years, such as 1996, 1998, 2006, 2010 and 2016. This would be due to the dynamic relationship between large-scale climatic indexes and other drivers of rainfall in the ARB.

4.4.2. The overall influence of SSTAs on the mRS rainfall changing-point

The change-point of rainfall for the entire ARB during the mRS was detected in 1997/98. The number of El Niño or La Niña events before and after 1997/98 was examined, and the number of El Niño events was almost the same, with four events both before and after the change-point. There were four La Niña events before the change-point and eight events after the change-point (Table 4). It is generally considered that La Niña increases the annual and MRS rainfalls, but decreases the mRS rainfall. Therefore, the higher number of La Niña events after the change-point can decrease the mRS rainfall, and partially affect the change-point. A high correlation of mRS rainfall with Nino3.4 was indeed detected after the change-point, which should be another indication of La Niña's influence on the mRS rainfall change-point. The mRS rainfall correlation with Nino3.4 was higher after the change-point, while the Nino3.4 correlation with the MRS was low (Table 4).

AMO and NTA correlations after the change-point were higher, especially in the mRS, but there was inconsistency for the annual and the MRS rainfall. The AMO correlations with the annual rainfall and MRS rainfall before the change-point were negative, but became positive after the change-point. A significant increasing trend of AMO SST in parallel with the ARB average temperature was observed. The change-point year of AMO SST was the same as the ARB mRS rainfall change-point. Therefore, AMO SST variability is the main role player in the ARB that reduces the mRS rainfall and generates a change-point. Moreover, after the mRS change-point, the temperature in both the AMO SST and ARB were significantly increased. Analogously with ENSO, the mRS rainfall correlation with AMO SST was also increased more after the change-point than before it. Overall, these findings show that the basin rainfall was more highly influenced by SST large-scale climate variability after the change-points than before them.

5. Conclusions

The variability, trend and change-point of temperature as well as rainfall were analyzed in Awash River basin (ARB) during 1986–2016 using different parametric and non-parametric statistical tests. In view of trend, the basin temperature showed a significant increasing trend on both an annual and seasonal basis. The ARB annual rainfall is non-significantly decreased. The entire ARB rainfall indicated a non-significant increasing trend during the major rainy season (MRS), while the minor rainy season (mRS) rainfall showed a significant decreasing trend. Furthermore, most of the stations that showed a

significant decreasing trend in rainfall were from the downstream parts of ARB. The mRS was revealed to have very high rainfall variability, especially in the downstream parts of ARB.

Change-point detection was also undertaken in this study, and in most of the times the annual and the MRS change-point in temperature was detected in 2001, whereas the mRS temperature change-point was found in 1997. There was no change-point found in the annual and MRS rainfalls. However, based on the BR and SNH tests, the mRS rainfall change-point was detected as having occurred in 1997/98, with an average rainfall of 267.6 mm before and 215.1 mm afterwards with a subsequent average rainfall decrease of 52.5 mm. The majority of stations in the downstream (lowland) portions of ARB showed a significant decreasing trend of rainfall. Likewise, change-point of rainfall were detected in the downstream parts of ARB. Similarly, all test types detected the annual and seasonal AMO SST change-point in 1997/98, which is the same year that the ARB rainfall change-point occurred for the mRS.

The correlation of DMI/IOD with rainfall was negative for the annual and seasonal series, implying that the warming phase of DMI leads to a decrease in rainfall in the ARB. Moreover, an El Niño year (1997) was followed by three La Niña years in 1998, 1999 and 2000 that resulted in four consecutive years of rainfall reduction in the downstream parts of the ARB where the mRS is the main contributor. Therefore, the change-point and decreasing trends in the mRS rainfall since 1997 can be attributed to the La Niña events. Additionally, the correlation of AMO with the mRS rainfall was negative, implying that a positive AMO reduced the mRS rainfall. Similarly, the correlation of NTA with the mRS was negative, implying that warming in the NTA would reduce the mRS rainfall. Overall, the mRS rainfall in the basin tended to decline with the increase in Indian and Atlantic Ocean SST, and there has been a constant SST increase since 2000.

For the most part, the average shift and a significant decreasing trend in rainfall, particularly in the mRS, should be attributed to the steady warming of the Indian and Atlantic Oceans, local warming, and La Niña events. More detailed studies of rainfall variability and climate change assessments would be very helpful, as rainfall variability has been a huge social and economic problem in the ARB. The mRS average rainfall shift, as well as a significant decreasing rainfall trend, should affect pre-agricultural land preparation, agricultural planning, and other related agricultural activities. Therefore, it is highly recommended to develop an early warning system for El Niño/La Niña events, to develop an appropriate water-management strategic plan, and to provide adaptation options for the local population.

Declarations

Author contribution statement

Yitea Seneshaw Getahun: Conceived and designed the experiments; Performed the experiments; Analyzed and interpreted the data; Contributed reagents, materials, analysis tools or data; Wrote the paper.

Ming-Hsu Li: Conceived and designed the experiments; Performed the experiments; Analyzed and interpreted the data; Wrote the paper.

Iam-Fei Pun: Performed the experiments; Analyzed and interpreted the data; Wrote the paper.

Funding statement

This research did not receive any specific grant from funding agencies in the public, commercial, or not-for-profit sectors.

Data availability statement

The datasets used in the study are available in the National Meteorological Agency (NMA) of Ethiopia repository. Access to NMA data can be allowed based on justifiable request.

The sea surface temperature anomalies (SSTAs) data were downloaded from NOAA as described in dataset section of this paper.

Declaration of interests statement

The authors declare no conflict of interest.

Additional information

No additional information is available for this paper.

Acknowledgements

The authors gratefully appreciate groups producing SST datasets such as Australian Bureau of Meteorology, Japan Agency for Marine-Earth Science and Technology (JAM- STEC), NOAA/NWS/CPC, NOAA/OAR/ESRL PSD and the Ethiopian National Meteorology Agency for providing observed meteorological datasets.

References

Abtew, W., Melesse, A.M., Dessalegne, T., 2009. El Niño NiNiño southern oscillation link to the blue nile river basin hydrology. Process 23, 3653–3660.

Adeba, D., Kansal, M.L., Sen, S., 2015. Assessment of water scarcity and its impacts on sustainable development in Awash basin, Ethiopia. Sustain. Water Resour. Manag. 1 (1), 71–87.

Asfaw, A., Simane, B., Hassen, A., Bantider, A., 2018. Variability and time series trend analysis of rainfall and temperature in northcentral Ethiopia: a case study in Woleka sub-basin. Weather Clim. Extrem. 19, 29–41.

Alemayehu, A., Bewket, W., 2017. Local spatiotemporal variability and trends in rainfall and temperature in the central highlands of Ethiopia. Geogr. Ann. Phys. Geogr. 99 (2), 85–101.

Apaydin, H.F., Kemal Sonmez, Yildirim, Y. Ersoy, 2004. Spatial interpolation techniques for climate data in the GAP region in Turkey. Clim. Res.

Bekele, D., Alamirew, T., Kebede, A., Zeleke, G., Melese, A.M., 2017. Analysis of rainfall trend and variability for agricultural water management in Awash River Basin, Ethiopia. J. Water Clim. Change 8 (1), 127–141.

Berhane, F., Zaitchik, B., Dezfuli, A., 2014. Subseasonal analysis of precipitation variability in the blue nile river basin. J. Clim. 27 (1), 325–344. https://journals.ametsoc.org/view/journals/clim/27/1/jcli-d-13-00094.1.xml.

Bisai, D., Chatterjee, S., Khan, A., B. N, 2014. Statistical analysis of trend and change-point in surface air temperature time series for midnapore weather observatory, West Bengal, India. J. Waste Water Treat. Anal. 5 (2).

Buishand, T.A., 1982. Some methods for testing the homogeneity of rainfall records. J. Hydrol. 58 (1-2), 11–27.

Borgomeo, E., Vadheim, B., Woldeyes, F.B., Alamirew, T., Tamru, S., Charles, K.J., Walker, O., 2018. The distributional and multi-sectoral impacts of rainfall shocks: evidence from computable general equilibrium modelling for the Awash basin, Ethiopia. Ecol. Econ. 146, 621–632.

Croitoru, A.E., Holobaca, I.H., Lazar, C., Moldovan, F., Imbroane, A., 2012. Air temperature trend and the impact on winter wheat phenology in Romania. Climatic Change 111 (2), 393–410.

Demissie, T.A., Sime, C.H., 2021. Assessment of the performance of CORDEX regional climate models in simulating rainfall and air temperature over southwest Ethiopia. Heliyon e07791.

Degefu, M.A., Rowell, D.P., Bewket, W., 2017. Teleconnections between Ethiopian rainfall variability and global SSTs: observations and methods for model evaluation. Meteorol. Atmos. Phys. 129 (2), 173–186.

Dibal, N.P., Mustapha, M., M, A.T., Yahaya, A.M., 2017. Statistical change-point Analysis in air temperature and rainfall time series for cocoa research institute of Nigeria, ibadan, Oyo state, Nigeria. Int. J. Appl. Math. Theor. Phys. 3 (4), 92.

Diro, G.T., Black, E., Grimes, D.I.F., 2008. Seasonal forecasting of Ethiopian spring rains. Meteorol. Appl. 15 (1), 73–83.

Dost, R., Obando, E.B., Hoogeveen, W., 2013. Water Accounting Plus (WA+) in the Awash River Basin Coping with Water Scarcity-Developing National Water Audits Africa Client: FAO, Land and Water Division. http://www.wateraccounting.org/files/projects/awash_basin.pdf. (Accessed 14 July 2019). Accessed.

Elsanabary, M.H., Gan, T.Y., 2015. Evaluation of climate anomalies impacts on the Upper Blue Nile Basin in Ethiopia using a distributed and a lumped hydrologic model. J. Hydrol. 530, 225–240.

Elzeiny, R., Khadr, M., Zahran, S., Rashwan, E., 2019. Homogeneity analysis of rainfall series in the upper blue nile river basin, Ethiopia. J. Eng. Res. 3 (September), 46–53.

Enyew, B.D., Steeneveld, G.J., 2014. Analysing the impact of topography on precipitation and flooding on the Ethiopian highlands. J. Geol. Geosci. 3, 173. https://www.longdom.org/open-access/analysing-the-impact-of-topography-on-precipitation-and-flooding-on-the-ethiopian-highlands-2329-6755-1000173.pdf.

Fekadu, K., 2015. Ethiopian seasonal rainfall variability and prediction using canonical correlation analysis (CCA). Earth Sci. 4 (3), 112.

Gali, S., 2015. On Importance of Normality Assumption in Using a T-Test: One Sample and Two Sample Cases, pp. 3–5.

Gedefaw, M., Wang, H., Yan, D., Song, X., Yan, D., Dong, G., Qin, T., 2018. Trend analysis of climatic and hydrological variables in the Awash river basin, Ethiopia. Water 10 (11), 1554.
Getahun, Y.S., Van Lanen, H.A.J., 2015. Assessing the impacts of land use-cover change on hydrology of melka kuntrie subbasin in Ethiopia, using a conceptual hydrological model. Hydrol. Curr. Res. 6 (3), 210, 2015.
Goovaerts, P., 2010. Combining areal and point data in geostatistical interpolation: applications to soil science and medical geography. Math. Geosci. 42, 535–554.
Gleixner, S., Keenlyside, N., Viste, E., Korecha, D., 2016. The El Niño effect on Ethiopian summer rainfall. Clim. Dynam. 49 (5–6), 1865–1883.
Hailu, R., Tolossa, D., Alemu, G., 2017. Water security: stakeholders' arena in the Awash river basin of Ethiopia. Sustain. Water Resour. Manag. 1–19.
Hayelom, B., Chen, Y., Marsie, Z., Negash, M., 2017. Temperature and precipitation trend analysis over the last 30 Years in southern tigray regional state, Ethiopia. (Accessed 25 April 2020).
Hare, W., 2003. Assessment of Knowledge on Impacts of Climate Change, Contribution to the Specification of Art, 2 of the UNFCCC WBGU (2003).
Hong, C.C., Li, T., Ho, T., Kug, J.C., 2008. Asymmetry of the Indian ocean dipole. Part I: observational analysis. J. Clim. 21 (18), 4834–4848 (2008).
IPCC, 2014. In: Pachauri, R.K., Meyer, L.A. (Eds.), Synthesis Report Summary for Policy Makers. Contribution of Working Groups I, II and III to the Fifth Assessment Report of the Intergovernmental Panel on Climate Change, Core Writing Team. IPCC, Geneva, Switzerland, p. 151. https://ar5-syr.ipcc.ch/ipcc/ipcc/resources/pdf/IPCC_SynthesisReport.pdf. (Accessed 11 August 2019).
IPCC, 2007. PCC Fourth Assessment Report: Climate Change 2007. Climate Change 2007: Working Group I: the Physical Science Basis. https://archive.ipcc.ch/publications_and_data/ar4/wg1/en/ch3s3-3-5.html. (Accessed 11 August 2021).
Jain, S.K., Kumar, V., Saharia, M., 2013. Analysis of rainfall and temperature trends in northeast India. Int. J. Climatol. 33 (4), 968–978.
Jaiswal, R.K., Lohani, A.K., Tiwari, H.L., 2015. Statistical analysis for change detection and trend assessment in climatological parameters. Environ. Process. 2 (4), 729–749.
Javari, M., 2016. Trend and homogeneity analysis of precipitation in Iran. Climate 4 (3), 44.
Kendall, M., 1975. Rank Correlation Methods. Charles Griffin, London. http://www.worldcat.org/title/rank-correlation-methods/oclc/489980698. (Accessed 11 May 2019). Accessed.
Korecha, D., Barnston, A.G., 2007. Predictability of june–september rainfall in Ethiopia. Mon. Weather Rev. 135 (2), 628–650.
Kuile, B.J. ter., 2009. The Relation between Temperature and Precipitation. http://www.srderoode.nl/Students/benjamin_internship_report.pdf. (Accessed 11 August 2021). Accessed.
Le, J.A., El-Askary, H.M., Allali, M., Sayed, E., Sweliem, H., Piechota, T.C., Struppa, D.C., 2020. Characterizing el Niño-southern oscillation effects on the blue Nile yield and the Nile river basin precipitation using empirical mode decomposition. Earth Syst. Environ. 4 (4), 699–711.
Lehmann, E.L., 1975. Nonparametrics, Statistical Methods Based on Ranks. Holden-Day Inc., Oakland, CA, USA.
Marchant, R., Mumbi, C., Behera, S., Yamagata, T., 2007. The Indian Ocean dipole ? the unsung driver of climatic variability in East Africa. Afr. J. Ecol. 45 (1), 4–16.
Marullo, S., Artale, V., Santoler, R., 2011. The SST multidecadal variability in the atlantic-mediterranean region and its relation to AMO. J. Clim. 24 (16), 4385–4401.
Mengistu, D., Bewket, W., Lal, R., 2014. Recent spatiotemporal temperature and rainfall variability and trends over the upper blue nile river basin, Ethiopia. Int. J. Climatol. 34 (7), 2278–2292.
Mann, H.B., 1945. Nonparametric tests against trend. Econometrica 13, 245–259.
Murendo, C., Keil, A., Zeller, M., 2010. Drought impacts and related risk management by smallholder farmers in developing countries: evidence from Awash River Basin, Ethiopia. Research in Development Economics and Policy (Discussion Paper Series). https://ideas.repec.org/p/ags/uhohdp/114750.html. (Accessed 14 May 2018). Accessed.
Mulugeta, S., Fedler, C., Ayana, M., 2019. Analysis of long-term trends of annual and seasonal rainfall in the Awash river basin, Ethiopia. Water 11 (7), 1498.
Ntwali, D., Ogwang, B.A., Ongoma, V., 2016. The impacts of topography on spatial and temporal rainfall distribution over Rwanda based on WRF model. Atmos. Clim. Sci. 6, 145–157.
Onyutha, C., Tabari, H., Taye, M.T., Nyandwaro, G.N., Willems, P., 2016. Analyses of rainfall trends in the nile river basin. J. hydro-environ. Res. 13, 36–51.
Onyutha, C., 2016. Variability of seasonal and annual rainfall in the River Nile riparian countries and possible linkages to ocean–atmosphere interactions. Nord. Hydrol 47 (1), 171–184. https://iwaponline.com/hr/article/47/1/171/1356/Variability-of-seasonal-and-annual-rainfall-in-the.
Onyutha, C., 2021. Graphical-statistical method to explore variability of hydrological time series. Nord. Hydrol 52 (1), 266–283 (2021). https://iwaponline.com/hr/article/52/1/266/78544/Graphical-statistical-method-to-explore.
Ogwang, B.A., Chen, H., Li, X., Gao, C., 2014. The influence of topography on East African October to December climate: sensitivity experiments with RegCM4. Advances in Meteorology. https://www.hindawi.com/journals/amete/2014/143917/.
Park, J.-H., Li, T., 2018. Interdecadal modulation of el niño–tropical North Atlantic teleconnection by the atlantic multi-decadal oscillation. Clim. Dynam. 1–16.
Pearson, K., 1920. Notes on the history of correlation. Biometrika 13 (1), 25–45. https://link.springer.com/article/10.1057/jt.2009.5.
Ros, F.C., Tosaka, H., Sasaki, K., Sidek, L.M., Basri, H., 2015. Absolute homogeneity test of Kelantan catchment precipitation series. In: AIP Conference Proceedings, 1660. AIP Publishing LLC, 050028. Accessed March 24, 2019).
Ramli, M.F., Aris, A.Z., Jamil, N.R., Aderemi, A.A., 2019. Evidence of climate variability from rainfall and temperature fluctuations in semi-arid region of the tropics. Atmos. Res. 224, 52–64.
Reeves, J., Chen, J., Wang, X.L., Lund, R., Lu, Q.Q., 2007. A review and comparison of change point detection techniques for climate data. J. Appl. Meteorol. Climatol. 46 (6), 900–915. https://journals.ametsoc.org/view/journals/apme/46/6/jam2493.1.xml.
Samy, A., Ibrahim M, G., Mahmod, W.E., Fujii, M., Eltawil, A., Daoud, W., 2019. Statistical assessment of rainfall characteristics in upper blue nile basin over the period from 1953 to 2014. Water 2019 (11), 468.
Spiegel, M.R., 1998. Theory and Problems of Statistics, Schaum's Outline Series, fifth ed. McGraw-Hill, New York, NY, USA http://www.fulviofrisone.com/attachments/article/447/Schaum's%20Outline%20of%20Statistic.pdf.
Segele, Z.T., Lamb, P.J., 2005. Characterization and variability of Kiremt rainy season over Ethiopia. Meteorol. Atmos. Phys. 89 (1–4), 153–180.
Sen, P.K., 1968. Estimates of the regression coefficient based on Kendall's tau. J. Am. Stat. Assoc. 63, 1379–1389.
Sahin, S., Cigizoglu, H.K., 2010. Homogeneity analysis of Turkish meteorological data set. Hydrol. Process. 24 (8), 981–992.
Spearman, C., 1904. The proof and measurement of association between two things. Am. J. Psychol. 15 (1), 72–101.
Suhaila, J., Yusop, Z., 2018. Trend analysis and change-point detection of annual and seasonal temperature series in Peninsular Malaysia. Meteorol. Atmos. Phys. 130 (5), 565–581.
Shawul, A., Chakma, S., 2020. Trend of extreme precipitation indices and analysis of long-term climate variability in the Upper Awash basin, Ethiopia. Theor. Appl. Climatol. 140 (1-2), 635–652.
Tadese, M.T., Kumar, L., Koech, R., Zemadim, B., 2019. Hydro-climatic variability: a characterisation and trend study of the Awash river basin, Ethiopia. Hydrology 6 (2), 35.
Tamiru, S., Tesfaye, K., Mamo, G., 2015. Analysis of rainfall and temperature variability to guide sorghum (sorghum bicolar) production in miesso areas, eastern Ethiopia. Int. J. Sustain. Agric. Res. 2 (1), 1–11.
Trenberth, K.E., Shea, D.J., 2006. Atlantic hurricanes and natural variability in 2005. Geophys. Res. Lett. 33, L12704.
Theil, H., 1950. A rank-invariant method of linear and polynomial analysis, part 3.Nederlandse Akademie van Wettenschappen. Proceedings 53, 1397–1412.
Tilahun, H., Erkossa, Teklu, Michael, M., Hagos, Fitsum, Awulachew, S.B., 2011. Comparative performance of irrigated and rainfed agriculture in Ethiopia. World Appl. Sci. J. https://cgspace.cgiar.org/handle/10568/41794.
Wedajo, G.K., Muleta, M.K., Gessesse, B., 2019. Spatiotemporal climate and vegetation greenness changes and their nexus for Dhidhessa River Basin, Ethiopia. Environ. Syst. Res. 8 (2019), 31.
Whitley, E., Ball, J., 2002. Statistics review 6: nonparametric methods. Crit. Care 6 (6), 509. (Accessed 10 May 2020).
Zarenistanak, M., Dhorde, A.G., Kripalani, R.H., 2014. Trend analysis and change-point detection of annual and seasonal precipitation and temperature series over southwest Iran. J. Earth Syst. Sci. 123 (2), 281–295.
Zaroug, M.A.H., Giorgi, F., Coppola, E., Abdo, G.M., Eltahir, E.A.B., 2014. Simulating the connections of ENSO and the rainfall regime of East Africa and the upper Blue Nile region using a climate model of the Tropics. Hydrol. Earth Syst. Sci. 18 (11), 4311–4323.
Zhao, W., Khalil, M.A.K., 1993. The relationship between precipitation and temperature over the contiguous United States. J. Clim. 6 (6), 1232–1236. https://journals.ametsoc.org/view/journals/clim/6/6/1520-0442_1993_006_1232_trbpat_2_0_co_2.xml.